Gradstein, F. M., Ludden, J. N., et al., 1992
Proceedings of the Ocean Drilling Program, Scientific Results, Vol. 123

41. REGIONAL CORRELATION OF MINERALOGY AND DIAGENESIS OF SEDIMENT FROM THE EXMOUTH PLATEAU AND ARGO BASIN, NORTHWESTERN AUSTRALIAN CONTINENTAL MARGIN[1]

John S. Compton,[2] David Mallinson,[2] Toedsit Netratanawong,[2] and Stanley D. Locker[2]

ABSTRACT

Correlation of mineral associations from sediment recovered on the northwestern Australian continental margin document the juvenile-to-mature evolution of a segment of the Indian Ocean. Lower Cretaceous sediments contain sandy-to-silty radiolarian claystone that consists of highly smectitic mixed-layered illite/smectite (I/S) in addition to minor amounts of diagenetic pyrite, barite, and rhodochrosite. These immature, poorly sorted sediments were derived from nearby continental margin sources. Discrete bentonite layers and abundant smectite are the alteration products of volcanic material deposited during early basin formation. Abundant quartz-replaced radiolarian tests suggest high surface-water productivity, and calcareous fossils indicate water depths were above the calcite compensation depth (CCD) in the juvenile Indian Ocean. The increase in pelagic carbonate from the mid- to Late Cretaceous signals the transition to mature, open-ocean conditions. Similar to other slowly deposited contemporaneous deep-sea sediments, mid- to Upper Cretaceous sediments of the northwestern margin of Australia contain palygorskite. This palygorskite is associated with calcareous sediment across the ooze-to-chalk transition, detrital mixed-layered I/S, and zeolite minerals in places. This palygorskite occurs above the transformation from opal-A to opal-CT. The underlying opal-CT sediment contains abundant smectite and zeolite minerals. Calcareous sediment dominates the Cenozoic, except at abyssal sites that were not inundated by calcareous turbidites. Paleocene and Eocene sediments contain abundant smectite and zeolite minerals derived from the alteration of volcanic material. Palygorskite was found to be associated with sepiolite and dolomite in Miocene sediments from Site 765 in the Argo Basin. Pliocene and Quaternary sediments contain detrital kaolinite and mixed-layered I/S, abundant opal-A radiolarian tests, and minor amounts of pyrite.

INTRODUCTION

The Australian and Indian continents started to drift apart during the Late Jurassic–Early Cretaceous break-up of Gondwanaland. One of the key objectives of ODP Legs 122 and 123 was to document the evolution of the passive Australian continental margin by examining its sedimentation history. During Legs 122 and 123, scientists recovered sediment from the Exmouth Plateau and the Argo Basin, and during DSDP Leg 27, they recovered sediment from the Argo, Gascoyne, Cuvier, and Perth abyssal plains adjacent to the continental margin of northwestern Australia (Fig. 1). Together these sites provide information about the rift-to-drift history along the northwestern continental margin of Australia and the juvenile-to-mature evolution of the Indian Ocean. This study examines the mineralogy of sediments recovered at Sites 261, 765, and 766, along with mineralogical data available from Leg 27 (Cooks et al., 1974) to establish regional depositional and diagenetic trends among the sites.

METHODS

Samples were collected on board the *JOIDES Resolution* during Leg 123 and samples from Site 261 were obtained from the ODP Core Repository. Bulk samples were scraped clean of any drilling mud contamination, placed in beakers with deionized water, and disaggregated with a rubber spatula. Dispersant (approximately 20 mL of 5 wt% sodium hexametaphosphate solution) was added to each sample to prevent flocculation of the clay minerals. The dispersed sample was placed in an ultrasonic bath for several minutes until the sediment particles had disaggregated and were suspended in a slurry. The slurry was washed through a 38-μm stainless-steel sieve and the collected >38-μm size fraction was dried overnight at 60°C. The <38-μm slurry was centrifuged to settle particles >2-μm in spherical diameter. The <2-μm slurry was centrifuged to settle particles >0.1 μm in diameter. The 0.1- to 2-μm size fraction typically consisted of a dark, greasy top layer (approximately <0.5 μm) and a light, sticky base layer. A glass smear slide was made for the >38 μm, 2 to 38 μm, <2 μm base

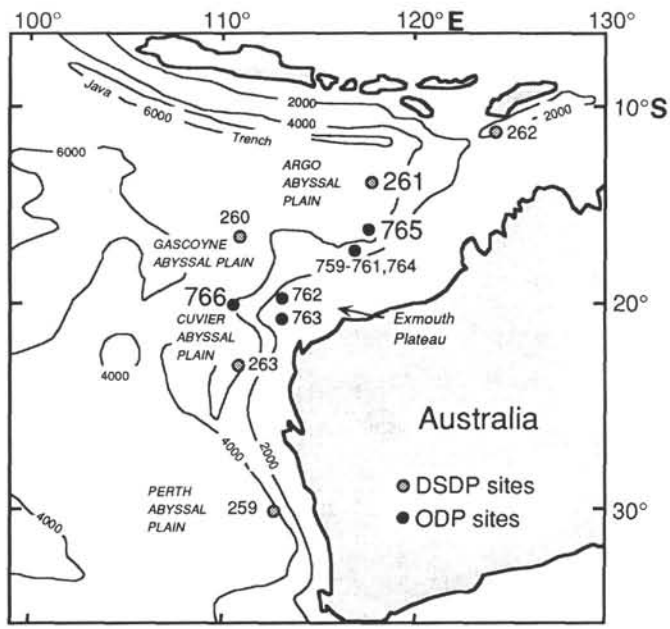

Figure 1. Location map of drill sites from DSDP Leg 27 and ODP Legs 122 and 123.

[1] Gradstein, F. M., Ludden, J. N., et al., 1992. *Proc. ODP, Sci. Results*, 123: College Station, TX (Ocean Drilling Program).

[2] Department of Marine Science, University of South Florida, St. Petersburg, FL 33701, U.S.A.

layer, and <2 μm top layer and analyzed using a Scintag XDS 2000 X-ray diffractometer (XRD) and Cu Kα radiation. The <2-μm size fraction was soaked in ethylene glycol overnight and analyzed using XRD. The percentage of interstratified illite in the mixed-layered I/S was determined by measuring the position of the glycolated 002/003 reflection and by using the techniques described by Reynolds and Hower (1970), Reynolds (1980), and Moore and Reynolds (1989). The relative abundance of the minerals was estimated from the integrated area of their most intense XRD peak (Tables 1 and 2; 0 = nondetectable, 1 trace [<1 wt%], and 6 = abundant [>20 wt%]).

MINERALOGY OF SEDIMENT FROM SITE 765

The mineralogy of Site 765 has been described in detail by Compton and Locker (this volume).

MINERALOGY OF SEDIMENT FROM SITE 766

The mineralogy of sediment from Site 766 can be divided into four distinct mineral associations, based primarily on differences in clay mineralogy. The relative abundance of the minerals at Site 766 is presented in Table 1, and the relationship among the mineral associations, sample location, sediment depth, age, and lithology is shown in Figure 2. Below, we describe the four different mineral associations from oldest to youngest.

Mineral Association IV

Mineral Association IV includes sediments from 454 to 230 meters below seafloor (mbsf) that are in contact with underlying diabase sills. We interpreted basement as intermediate between oceanic and continental (Ludden, Gradstein, et al., 1990). Sediments from mineral Association IV range in age from latest (?)Valanginian to Aptian and correspond to lithologic Unit III and the lowermost portion of lithologic Subunit IID (Fig. 2). The basal lithologic Subunit IIIB consists of greenish-gray to black, clayey siltstone and sandstone and is overlain by lithologic Subunit IIIA, which consists of greenish-gray to black porcelaneous claystone. The clay mineralogy of mineral Association IV is predominantly highly smectitic, randomly interstratified I/S. The I/S generally contains less than 10% illite layers; however, the I/S of two samples was found to contain about 25% illite layers. Minor-to-trace amounts of illite, kaolinite, and mica are common in the coarse clay size fraction (1–2 μm). Pyrite framboids and dolomite occur in places, but calcite is present only in trace amounts. The sediment from lithologic Subunit IIIB contains abundant silt and sand-sized grains consisting of quartz, feldspar (approximately equal amounts of K-feldspar and plagioclase feldspar), and lithic fragments. Zeolite minerals (predominantly clinoptilolite) were observed in sediments from 288 to 308 mbsf and from 241 to 251 mbsf. Quartz-replaced radiolarian tests are common in Hauterivian sediment, and opal-CT is abundant in the overlying Barremian to Aptian porcelaneous claystone. Mineral Association IV contains significantly more organic carbon than the overlying mineral associations, with organic carbon contents as high as 1.5 wt% (Ludden, Gradstein, et al., 1990).

Mineral Association III

Mineral Association III (80–192 mbsf) corresponds to lithologic Unit II, which consists of nannofossil ooze and clayey chalk that ranges in age from Aptian/Albian to Maestrichtian/Paleocene. The transition between mineral Associations IV and III is marked by a zone of poor recovery (192–230 mbsf). Mineral Association III contains the clay minerals palygorskite, I/S, and lesser amounts of illite. The I/S contains between 15% and 50% illite layers. Kaolinite occurs in the uppermost part of mineral Association III. Silt-sized quartz, feldspar, and mica grains are common. The calcite content increases and the organic carbon content decreases dramatically going from mineral Association IV to mineral Association III. Clinoptilolite is common in trace-to-minor amounts, but pyrite and dolomite were not observed. Trace amounts of opal-CT were observed in the lower half of mineral Association III.

Mineral Association II

Mineral Association II occurs in Paleocene and Eocene nannofossil ooze from 28 to 67 mbsf; it contains I/S, kaolinite, illite, and possibly trace amounts of palygorskite and mica. The I/S contains between 10% and 25% illite layers. Zeolite and dolomite are common in trace amounts. Mineral Association II corresponds to lithologic Subunit IB, which consists of pale brown to white, highly calcareous nannofossil ooze (>90 wt% calcite).

Mineral Association I

Mineral Association I (22–0 mbsf) corresponds to highly calcareous nannofossil ooze of lithologic Subunits IA and the uppermost portion of IB that range in age from Pliocene to Quaternary. The clay mineralogy consists of I/S, a noticeable increase in the kaolinite content, minor amounts of illite, and possibly trace amounts of palygorskite. The I/S contains approximately 40% illite layers. Opal-A radiolarian tests and trace amounts of pyrite were also observed in mineral Association I.

MINERALOGY OF SEDIMENT FROM SITE 261

The mineralogy of sediment from Site 261 was originally described by Cooks et al. (1974). Additional samples from Site 261 were included in this study to determine the mineral associations more accurately and to compare the mineralogy of Sites 261 and 765 (Compton and Locker, this volume). Site 261 is located 4°N of Site 765 in the Argo Basin, and together these two sites provide a comparison of sedimentation and diagenetic histories across the Argo Basin that can be correlated from continuous seismic profiles between the two sites (Buffler, 1990). The relative abundance of the minerals found at Site 261 are listed in Table 2. The relationships among sediment depth, sample location, age, lithologic units, and mineral associations (defined below from oldest to youngest) are shown in Figure 3. The recently revised biostratigraphic age dates of sediment from Site 261 are used in Figure 3 (Dumoulin and Bown, this volume).

Mineral Association V

The basal sediments (448–524 mbsf) at Site 261 are Tithonian to Hauterivian/Valanginian in age. These sediments are in contact with oceanic basalt. Mineral Association V corresponds to lithologic Unit IV, which consists of claystone that contains quartz-replaced radiolarian tests, quartz sand and silt, and, in places, abundant barite and calcite. The sand, silt, and coarse clay size fractions (>1 μm) contain quartz and some minor K-feldspar, discrete illite, and trace amounts of kaolinite. The clay fraction is dominated by I/S that contains <10% illite layers, with the exception of the basal sediments, which contain I/S that has about 20% illite layers.

Mineral Association IV

Mineral Association IV (363–438 mbsf) corresponds to the base of lithologic Unit III, which consists of quartz-replaced radiolarian tests and quartz-sandy and silty claystones of Barremian age. These sediments are composed predominantly of quartz, but also contain I/S and trace amounts of K-feldspar, plagioclase feldspar, illite, and kaolinite. The I/S contains approximately 20% to 30% illite layers, which distinguishes mineral Association IV from mineral Association V.

Table 1. Mineralogy of sediments recovered at Site 766.

M.A.	Core	Section	cm	Depth (mbsf)	Color	Lithology	Silica			Carbonate			Feldspar		Mica	Clay Minerals <2µm					Pyr	Zeol
							Qtz	O-A	O-CT	Wt. % CaCO3	Calcite	Dolo	K	Plag		Illite	Kaol	Palyg	I/S	%I		
	1R	1	147-150	1.47	Red/brown	Siliceous nannofossil ooze	4	4	0	80.4	6	0	3	0	0	1	3	1	4	?	1	0
I	2R	3	145-150	12.15	Orange/brown	Siliceous nannofossil ooze	4	0	0	62.6	6	0	0	0	0	2	4	0	4	40	1	0
	3R	3	145-150	21.75	Tan/orange	Siliceous nannofossil ooze	2	0	0	94.0	6	0	0	0	1	1	3	1	4	40	0	0
	4R	1	145-150	28.45	Tan/white	Siliceous nannofossil ooze	1	0	0	95.8	6	0	0	1	0	2	1	1	4	10	0	1
	6R	3	145-150	50.75	Tan/white	Siliceous nannofossil ooze	1	0	0	92.8	6	0	0	0	0	2	2	0	4	10	0	1
II	7R	6	80-82	54.30	Tan/white	Siliceous nannofossil ooze	1	0	0	-	6	2	0	0	1	1	2	0	5	?	0	0
	8R	1	145-150	67.15	Tan/white	Siliceous nannofossil ooze	0	0	0	94.9	6	1	0	0	0	1	2	1	4	25	0	1
	9R	3	145-150	79.75	Yellow/brown	Siliceous nannofossil ooze	1	0	0	94.1	6	0	0	0	0	1	2	2	3	45	0	0
	11R	4	107-112	100.27	Tan	Siliceous nannofossil ooze	2	0	0	-	6	0	0	1	1	1	2	3	4	?	0	0
	12R	1	145-150	105.75	Tan/white	Siliceous nannofossil ooze	1	0	0	90.8	6	0	0	1	0	1	2	3	4	?	1	0
	13R	2	77-80	116.17	Brown	Siliceous nannofossil ooze	2	0	0	-	3	0	2	1	0	1	2	6	5	50?	0	0
	15R	3	140-150	137.60	Tan/brown	Clayey chalk	2	0	0	60.6	6	0	0	1	0	2	0	5	5	45	0	1
III	17R	4	35-37	157.35	Drk brown	Clayey chalk	2	0	0	-	4	0	0	0	0	2	0	5	5	50	0	1
	18R	3	140-150	166.50	Tan	Clayey chalk	2	0	1	53.2	5	0	1	0	1	2	0	5	5	50	0	1
	19R	3	136-140	176.06	Brown	Clayey chalk	3	0	1	-	6	0	1	1	0	2	0	5	5	40	0	2
	20R	3	55-59	184.95	Tan	Clayey chalk	1	0	1	-	6	0	0	0	0	1	0	3	4	15	0	1
	21R	1	53-58	191.53	tan	Clayey chalk	2	0	0	-	4	0	1	1	1	2	0	4	5	25	0	1
	25R	1	23-26	229.83	Pale green	Siliceous claystone	1	0	3	-	4	0	0	0	1	2	0	0	6	<10	0	0
	26R	1	140-150	240.70	Green/tan	Siliceous claystone	3	0	3	1.2	1	0	1	1	1	2	0	0	6	<10	0	4
	27R	2	68-72	251.08	Pale green	Porcellaneous claystone	2	0	5	-	2	0	1	1	1	1	1	0	5	<10	0	1
	28R	6	103-106	267.13	Drk brown/gray	Porcellaneous claystone	2	0	5	-	2	0	1	1	1	2	1	0	5	<10	1	0
	29R	4	95-97	273.75	Gray/brown	Porcellaneous claystone	3	0	5	-	1	0	0	1	1	2	1	0	5	<10	0	0
	30R	1	140-150	279.30	Gray/black	Porcellaneous claystone	4	0	5	4.1	2	2	2	1	1	3	1	0	6	<10	0	0
	31R	1	54-57	288.04	Drk brown/gray	Porcellaneous claystone	4	0	5	-	2	0	0	0	1	3	1	0	6	25?	1	2
IV	32R	4	130-132	303.00	Drk brown/black	Clayey siltstone	4	0	0	-	0	0	0	0	1	2	1	0	6	<10	1	2
	33R	1	140-150	308.20	Drk brown	Silty claystone	3	0	0	1.0	1	2	1	1	1	3	1	0	6	<10	0	2
	36R	1	134-138	337.14	Drk brown	Silty claystone	3	0	0	-	1	2	0	0	0	2	1	0	6	<10	0	0
	37R	1	140-150	346.90	Drk green	Clayey siltstone	4	0	0	-	1	2	1	0	1	3	1	0	6	<10	1	1
	38R	3	96-98	359.06	Drk brown	Clayey siltstone	4	0	0	-	1	0	1	0	1	2	2	0	6	25?	0	0
	40R	3	140-150	378.90	Drk green/black	Silty claystone	2	0	0	15.1	2	0	1	1	1	1	3	0	6	<10	0	0
	43R	3	140-150	407.90	Brown/blk	Silty claystone	3	0	0	3.2	1	2	1	1	1	1	1	0	6	<10	1	0
	46R	4	140-150	438.40	Black	Clayey siltstone	4	0	0	4.3	1	2	1	0	1	2	1	0	6	<10	1	0
	48R	2	118-122	454.48	Green/blk	Claystone	0	0	0	-	0	0	0	1	0	1	0	0	6	<10	0	0

M.A. = mineral association; Qtz = quartz; O-A = opal-A; O-CT = opal-CT; Dolo = dolomite; K = potassium feldspar; Plag = plagioclase; Kaol = kaolinite; Palyg = palygorskite; I/S = illite/smectite; %I = % illite layers in I/S; Pyr = pyrite; Zeol = zeolite. Integers 0 through 6 indicate relative mineral abundance from peak areas: 0 = nondetectable; 1 = trace (≤1 wt%); 6 = abundant (≥20 wt%).

Table 2. Mineralogy of sediments recovered at Site 261.

M.A.	Core	Section	cm	Depth (mbsf)	Color	Lithology	Silica			Carbonate			Feldspar		Mica	Clay Minerals <2μm					Bar	Pyr	Zeol
							Qtz	O-A	O-CT	Calcite	Dolo	Sid	K	Plag		Illite	Kaol	Palyg	I/S	%I			
	2R	1	119	10.69	Mottled, gray brown	Siliceous clay	3	3	0	1	0	0	2	2	0	3	2	0	6	30-40	0	1	0
	2R	2	80	11.8	Brown	Siliceous clay	3	3	0	0	0	0	1	1	1	3	2	0	6	30?	0	1	0
I	3R	1	125	48.75	Mottled, brown gray	Carbonate-silty clay	2	0	0	1	1	0	0	0	3	2	5	0	5	20?	0	0	1
	3R	4	94	52.94	Gray brown	Clay	3	0	0	0	0	0	2	2	3	4	5	0	6	25?	0	0	0
	4R	2	116	97.66	Gray brown	Silty clay	3	0	0	0	0	0	3	1	3	4	5	0	6	30?	0	0	0
	5R	1	134	162.94	Mottled brown orange	Silty clay	3	0	0	0	0	1	2	2	2	3	1	3	6	30?	0	1	0
	6R	1	77	171.77	Mottled brown orange	Silty clay	3	0	0	0	0	1	4	2	0	3	1	3	6	54	0	1	0
II	6R	3	89	174.89	Brown	Silty clay	5	0	0	1	0	1	2	2	0	3	1	3	6	50	1	1	0
	7R	3	87	184.37	Brown	Sandy, silty clay	5	0	0	0	0	0	2	2	2	4	1	3	6	40-44	1	0	0
	8R	4	122	195.72	Brown	Zeolitic, sandy, silty clay	4	0	0	0	0	0	3	2	0	3	1	3	6	44	0	0	4
	9R	3	114	203.94	Mottled brown orange	Zeolitic, sandy, silty clay	2	0	3	0	0	1	3	4	1	3	0	0	6	10	0	0	5
	12R	2	38	229.88	Gray green	Barite-rich clay	3	0	3	0	0	1	2	2	0	3	1	0	4	<10	6	0	1
	14R	1	20	247.2	White gray	Barite-rich clay	4	0	3	1	1	0	2	2	3	3	0	0	6	<10	5	1	0
III	16R	1	118	267.18	Gray green	Gypsum-rich, silty clay	3	0	3	0	0	0	2	2	0	3	1	2	6	<10	1	1	0
	18R	1	136	286.36	Mottled gray green black	Sandy, silty clay	6	0	3	0	1	0	1	1	0	2	1	0	5	<10	0	0	0
	19R	3	62	307.62	Mottled green gray black	Sandy, silty clay	6	0	1	1	1	0	1	1	0	2	1	0	4	<10	0	0	0
	21R	2	104	335.04	Gray	Sandy, silty clay	6	0	0	1	0	0	1	0	0	1	0	0	3	10	1	1	0
	23R	2	70	363.2	Gray green	Sandy, silty clay	6	0	0	1	0	0	0	0	0	1	1	0	2	20?	0	0	0
IV	24R	2	110	382.6	Gray green, laminated	Sandy, silty clay	6	0	0	0	0	0	1	0	0	1	1	0	3	23	0	0	0
	26R	2	52	420.02	Gray laminated	Sandy, silty clay	6	0	0	0	0	0	0	0	0	1	1	0	2	?	0	1	0
	27R	1	70	437.7	Orange brown	Sandy, silty clay	6	0	0	0	0	0	1	1	0	1	1	0	2	30	1	1	0
	28R	2	39	448.39	Mottled orange brown	Sandy, carbonate-silty clay	4	0	0	6	0	0	1	1	0	1	1	0	3	<10	1	1	0
	29R	2	130	468.3	Pale red	Sandy, silty clay	6	0	0	0	0	0	0	0	0	1	0	0	3	<10	2	1	0
V	30R	1	126	485.76	Brown	Barite-rich, sandy, silty clay	5	0	0	0	0	1	1	0	1	2	1	0	5	<10	6	1	0
	31R	3	66	507.16	Red brown	Barite-rich, sandy, silty clay	4	0	0	0	0	0	1	0	0	1	0	0	2	20	6	1	0
	32R	2	17	524.17	Mottled red brown white	Sandy, carbonate-silty clay	5	0	0	5	0	0	1	0	0	2	1	0	5	25	1	1	0

M.A. = mineral association; Qtz = quartz; O-A = opal-A; O-CT = opal-CT; Dolo = dolomite; Sid = siderite; K = potassium feldspar; Plag = plagioclase; Kaol = kaolinite; Palyg = palygorskite; I/S = illite/smectite; %I = % illite layers in IS; Bar = barite; Zeol = zeolite. Integers 0 through 6 indicate relative mineral abundance from peak areas; 0 = nondetectable; 1 = trace (≤1 wt%); 6 abundant (≥20 wt%).

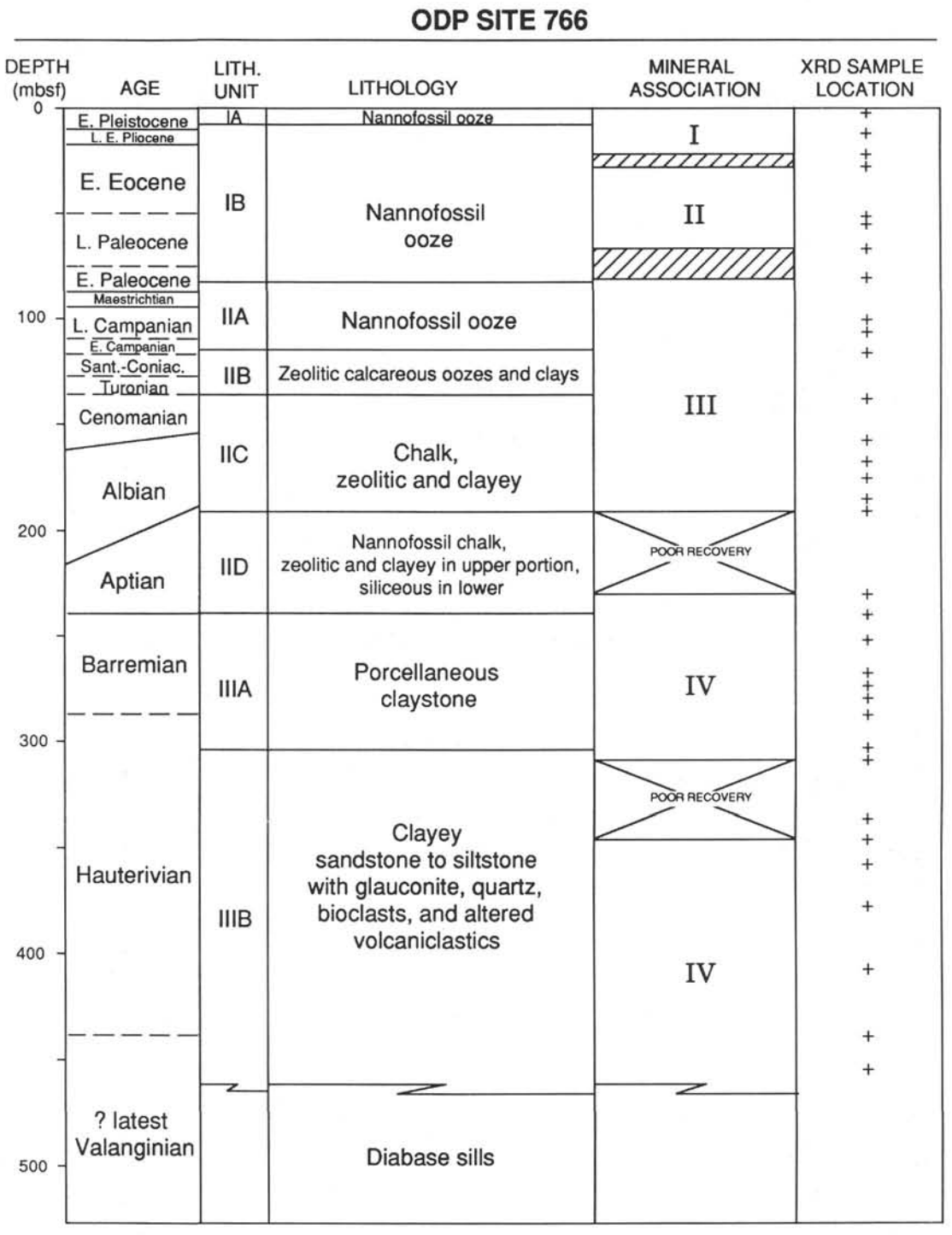

Figure 2. Correlation among sediment depth, age, lithology, mineral associations, and sample location of sediment from Site 766. Stippled area denotes transition between mineral associations.

Mineral Association III

Mineral Association III (204–335 mbsf) corresponds to the upper portion of lithologic Subunit IIIB. Lithologic Subunit IIIB consists of opal-CT radiolarian-rich claystone and is Aptian to Cenomanian in age. The clay mineralogy is dominated by I/S that contains <10% illite layers. Discrete illite is common, and kaolinite was found in trace amounts. In places, the claystone contains abundant zeolite minerals (mostly clinoptilolite) and barite (Table 2).

Mineral Association II

Mineral Association II (163–196 mbsf) corresponds to lithologic Subunit IIIA, which consists of quartz-sandy and silty claystones and is Turonian to late Campanian in age. The clay minerals include I/S, palygorskite, illite, and trace amounts of

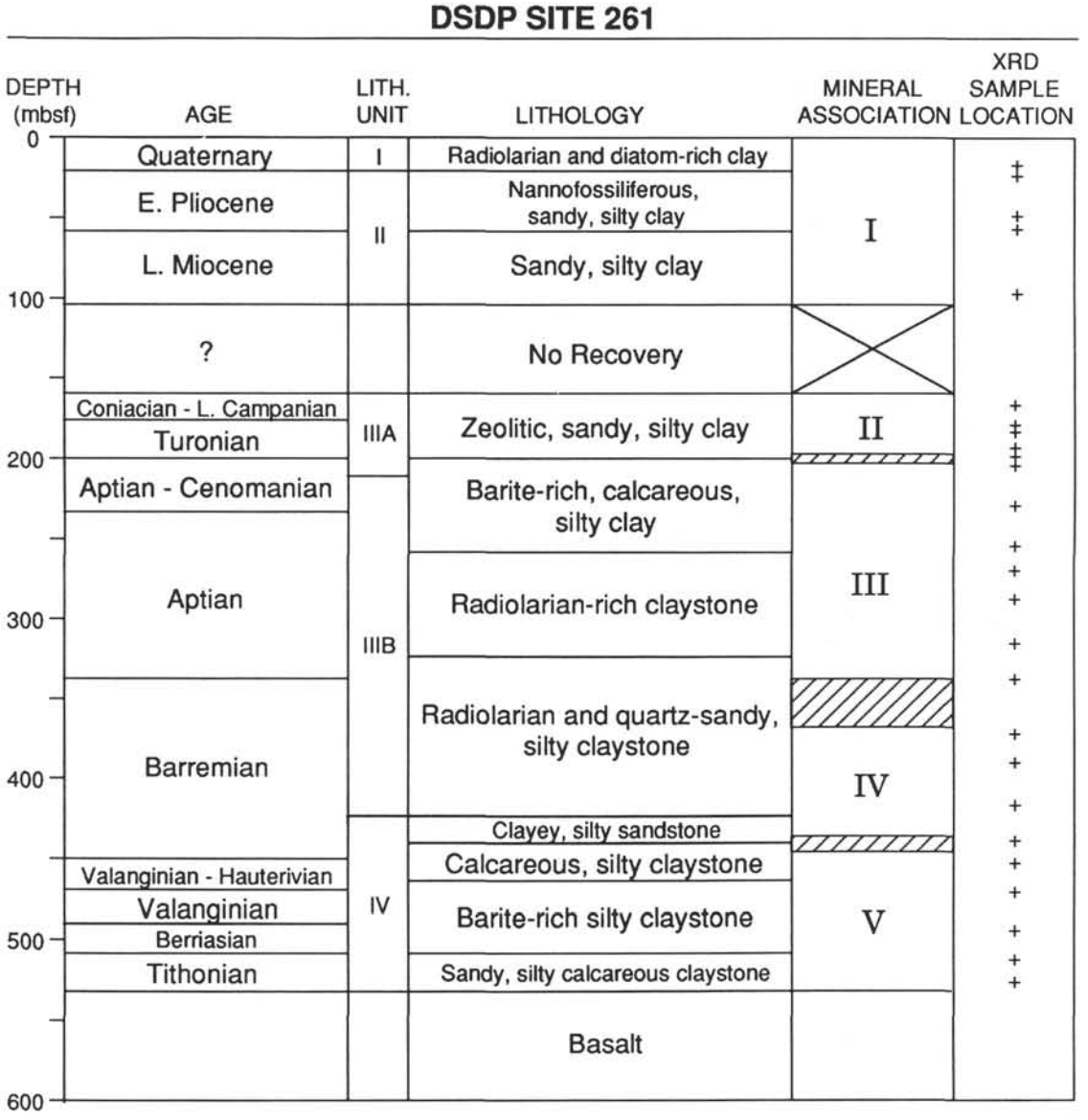

Figure 3. Correlation among sediment depth, age, lithology, mineral associations, and sample location of sediment from Site 261. Stippled area denotes transition between mineral associations.

kaolinite. The I/S contains 30% to 54% illite layers. Trace amounts of siderite were observed in the upper half of mineral Association II, and zeolite minerals were found in the basal sediments of mineral Association II.

Mineral Association I

Mineral Association I (0–98 mbsf) corresponds to lithologic Units I and II, which consists of quartz-sand silty and siliceous clays that are late Miocene to Quaternary in age. The clay minerals consist of I/S, kaolinite, illite, and mica. The I/S contains approximately 20% to 40% illite layers. Kaolinite and mica are significantly more abundant in mineral Association I. Trace amounts of calcite occur as nannofossils in the Pliocene sediment, and biogenic silica (opal-A) occurs in the Quaternary sediment.

DIAGENETIC TRENDS

The generalized diagenetic sequence observed with increasing burial depth in sediment recovered from the northwestern Australian margin is summarized in Figure 4. The uppermost Quaternary-to-Pliocene sediment contains diagenetic pyrite, but is dominated by pelagic carbonate sediment that contains biogenic silica (opal-A), volcanic glass, detrital I/S, kaolinite, mica, quartz, and feldspar. Miocene sediment is absent or present in minor amounts at most of the sites, except at Site 765, where the sediment contains diagenetic palygorskite, sepiolite, and dolomite (Compton, this volume; Compton and Locker, this volume). Eocene-to-Paleocene sediment contains highly smectitic I/S, associated with zeolite minerals that were probably derived from the alteration of volcanic material.

Albian-to-Maestrichtian sediment contains palygorskite, associated with I/S having 20% to 50% illite layers. The Upper Cretaceous palygorskite generally occurs within the calcareous ooze-to-chalk transformation. The transition to more calcareous-rich, mid- to Upper Cretaceous sediment is preceded by an opal-CT silica-rich interval at most sites. The underlying mid-Cretaceous (Albian to Aptian) opal-CT porcelaneous mudstone contains smectitic I/S and clinoptilolite. The opal-A-to-opal-CT transformation occurs immediately below the Upper Cretaceous

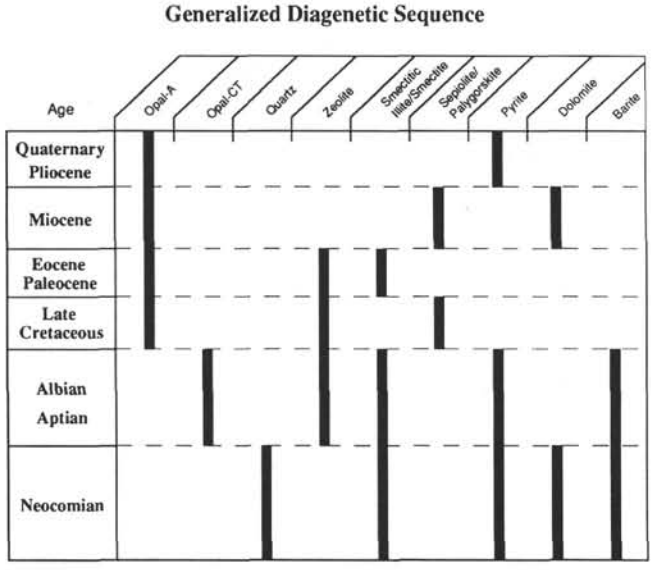

Figure 4. Generalized diagenetic sequence that was observed for sediments on the western Australian continental margin.

palygorskite-bearing sediment. The underlying Neocomian sediment is generally coarser-grained (silty and sandy claystone) and is also highly smectitic, but the opal-CT has been transformed to diagenetic quartz. The diagenetic minerals pyrite, barite, dolomite, and rhodochrosite also were commonly observed in trace to minor amounts.

Clay Mineral Diagenesis

Origin of I/S. A detrital vs. diagenetic origin of the mixed-layered I/S is differentiated here on the basis of the percentage of illite layers. I/S containing highly variable and abundant illite layers is most likely detrital in origin because, for the most part, these sediments have not been exposed to a sufficiently high diagenetic grade (temperature) to produce the systematic increase in illite layers predicted during the illitization reaction (e.g., Perry and Hower, 1970; Hower et al., 1976; Eberl and Hower, 1976). It is possible that the illitization reaction is occurring in the basal sediments at Sites 765 and 261, where the percent illite layers increase from <10% to 20% or 40% (Compton and Locker, this volume). The temperature of these basal sediments is considerably lower than the temperature observed for the illitization reaction in Miocene sediment from the Gulf Coast region of the U.S. (Hower et al., 1976) and the Miocene Monterey Formation in California (Compton, in press). However, the illitization reaction may have occurred at these lower temperatures over the much longer time available to these Upper Jurassic/Lower Cretaceous sediments. In contrast to detrital I/S, I/S derived from the alteration of volcanic ash is distinguished by its uniform, highly smectitic composition, with generally <10% illite layers. Alteration of volcanic material to highly smectitic I/S can occur *in situ* (e.g., bentonite layers or disseminated ash) or during weathering of continental volcanic rocks. Several bentonite layers composed of nearly 100% smectite clay minerals were identified from Sites 761, 765, and 766 (von Rad and Thurow, in press). Based on the abundance of highly smectitic I/S, volcanism on the northwestern Australian margin appears to have been most active in Early to mid-Cretaceous time and possibly during Paleogene time.

Origin of Palygorskite. Palygorskite occurs in Upper Cretaceous sediments from Sites 259, 260, 261, 765, and 766. Palygorskite is also abundant in the Miocene sediment from Site 765 and has been reported from Miocene sediment recovered at Site 260 (Gascoyne Abyssal Plain; Cooks et al., 1974). Palygorskite was not observed in upper Miocene sediment recovered at Site 261. The Miocene palygorskite at Site 765 appears to be authigenic, based on its fibrous growth within the sediment pore spaces and on the depletion of pore-water Mg at sediment depths containing abundant palygorskite (Compton and Locker, this volume). Upper Cretaceous palygorskite at Sites 259, 260, 261, 765, and 766 is associated with clayey calcareous sediment that contains significant amounts of zeolite minerals. The I/S associated with the palygorskite has been inferred as detrital, based on its highly variable and large percentage of illite layers. Below, and in places somewhat overlapping with the base of the palygorskite-bearing sediment, opal-A transforms to opal-CT, and the zeolite abundance increases. For example, at Site 766, the palygorskite occurs in the transition from calcareous ooze to chalk and is underlain by opal-CT rocks. Zeolite minerals occur in the lower half of palygorskite-bearing mineral Association III and in the underlying highly smectitic, opal-CT sediment of mineral Association IV (Fig. 2). A similar sequence was observed in the far less calcareous Upper Cretaceous sediment from Sites 261 and 765; palygorskite and detrital I/S occur above the sediment interval that contains opal-CT and highly smectitic I/S.

Palygorskite is a Mg-rich aluminosilicate that can be either detrital or authigenic (see review by Kastner, 1981). Palygorskite has been most commonly observed in Upper Cretaceous deep-sea sediments that are associated with silica-rich minerals, such as opal-CT, zeolite, and smectite (Berger and von Rad, 1972; von Rad and Rösch, 1972; von Rad et al., 1977). Textural evidence of delicate, fibrous palygorskite growing on mineral surfaces in association with other diagenetic, silica-rich minerals strongly suggests an authigenic origin for much of the palygorskite observed in marine sediment. Volcanic ash, biogenic silica, and smectite have been suggested as possible precursors to palygorskite formation (Peterson et al., 1970; von Rad and Rösch, 1972), and palygorskite tends to be associated with slow sedimentation rates and hiatuses (Couture, 1977). The concentration of palygorskite in Upper Cretaceous deep-sea sediment has been attributed to the deposition of silica-rich sediment, slow sedimentation rates, and increased volcanic activity (Kastner, 1981). A detrital origin for marine palygorskite has been suggested for the west African margin (Chamley and Millot, 1975) and the continental shelf of the southeastern U.S. (Weaver and Beck, 1977). These authors proposed that the palygorskite formed in nearshore alkaline lakes and that the palygorskite was later reworked into marine deposits.

The palygorskite in Upper Cretaceous sediment from the northwestern margin of Australia is generally associated with zeolite minerals and biogenic silica (opal-A), but is not directly associated with opal-CT or highly smectitic I/S. The palygorskite occurs directly above the sediment interval that contains abundant opal-CT, as well as zeolite and smectite minerals, and is overlain by zeolitic, smectite-rich Paleocene sediment. This sequence was observed at all of the sites studied, except Site 263 (Fig. 4). The source of the silica that formed authigenic palygorskite may have been from the solution of biogenic silica. Radiolarian tests are barren to rare in palygorskite-bearing Upper Cretaceous sediment at Sites 765 and 766, but pore-water silica ranges from 300 to 600 µm and from 200 to 800 µm in palygorskite sediment at Sites 765 and 766, respectively (Ludden, Gradstein, et al., 1990). The silica concentration may be an important control on the silica-rich mineral that precipitates. If the silica concentration is high, as in sediment containing abundant biogenic silica or altered volcanic ash, then opal-CT precipitation may remove silica and prevent palygorskite precipitation. The lower silica concentration of less siliceous sediments may result in pore waters being undersaturated with opal-CT, but supersaturated with palygorskite. Mg was probably derived from pore water and from diffusion of Mg ions

from the overlying seawater. Slow sedimentation rates should allow significant amounts of Mg to diffuse from the overlying seawater. The removal of pore-water Mg during palygorskite precipitation may have inhibited the opal-A-to-opal-CT transformation (Kastner et al., 1977) and may explain why opal-CT occurs in sediment below the sediment interval that contains palygorskite at all of the sites studied. In addition, Mg uptake during the alteration of volcanic material to smectite may have removed pore-water Mg and may explain why palygorskite is not directly associated with highly smectitic I/S at these sites.

Silica Diagenesis

The recrystallization of biogenic silica (opal-A) to opal-CT (nomenclature of Jones and Segnit, 1971) and then to quartz with increasing burial depth, observed in many deep-sea sediments (e.g., Kastner, 1981), also was observed at sites on the northwestern margin of Australia. The uppermost Quaternary sediments at these sites contain abundant, well-preserved, opal-A radiolarian tests (Ludden, Gradstein, et al., 1990). Radiolarian tests composed of opal-A, or recrystallized to opal-CT or quartz, are common throughout Cretaceous sediments, but biogenic silica is largely absent from Tertiary sediments on the Australian margin. At Site 766, the silica transformations correspond to zones of poor recovery because of the presence of hard porcellanite and chert. The abundance and mineralogy of radiolarian tests correlate well with the pore-water silica concentrations (Compton and Locker, this volume). The pore-water silica concentration decreases in the sediment interval where opal-A transforms to opal-CT from about 800 μM to between 200 and 600 μM. Silica concentrations decrease to about 100 to 200 μM in the sediment interval where opal-CT transforms to diagenetic quartz. Age of the sediment appears to be equally or more important than temperature for determining the timing of the silica transformations at these sites, based on the relatively low present-day geothermal gradient of the passive Australian continental margin (around 32°C/km) and the shallow burial depths (<1 km). The sediment composition, particularly the clay mineral content, may have also affected the timing of the silica transformations, as discussed above (Kastner et al., 1977; von Rad et al., 1977). The generally abundant radiolarian tests present in Lower to mid-Cretaceous sediments may indicate high surface-water productivity that resulted from fluvial nutrient influx or upwelling in the presumably narrow, restricted basin of the incipient Indian Ocean. Radiolarian tests are particularly abundant in sediment from Site 261. Barite ($BaSO_4$) is abundant in several samples from Sites 261 and 765 from sediment intervals rich in radiolarian tests, and high Ba contents were found in bulk radiolarite samples from Site 765 (Plank and Ludden, this volume). Ba is commonly associated with siliceous, clay-rich sediment that was deposited below regions of high surface productivity (e.g., Schmitz, 1987). Seawater has abundant sulfate, and although some of this sulfate may have been reduced to sulfide (see below), apparently sufficient sulfate was available to precipitate barite. The solution of biogenic silica is evident in the commonly observed molds of radiolarian tests, particularly in sediment that contains relatively small amounts of biogenic silica (Dumoulin, this volume). The opal-A radiolarian tests apparently dissolved before they were replaced by opal-CT or quartz (von Rad et al., 1977).

Zeolite Formation

The most common zeolite mineral at the sites investigated is clinoptilolite; no phillipsite was observed. Clinoptilolite is most common in Upper Cretaceous deep-sea sediments (Kastner, 1981), where it typically occurs as discrete crystals associated with radiolarian tests (Berger and von Rad, 1972). Zeolite minerals have also been documented to form from the alteration of volcanic ash (e.g., Hay, 1963; Iijima, 1978). The association of zeolite minerals with sediment that contains highly smectitic I/S in Upper Cretaceous sediments from Sites 261, 765, and 766, suggests that some of the clinoptilolite formed by alteration of volcanic ash. Zeolite precipitation may also have been promoted by high pore-water silica concentrations from the solution of biogenic silica, as suggested by clinoptilolite molds of radiolarian tests. Clinoptilolite has been more commonly observed associated with partially dissolved siliceous fossils than with volcanic material (Riech and von Rad, 1979). Zeolite minerals are more abundant in calcareous sediment on the Australian margin than in the underlying smectite- and radiolarian-rich Neocomian sediment, which supports the observation that clinoptilolite precipitation may be enhanced in carbonate-rich sediments (Stonecipher, 1976). Clinoptilolite is most abundant in the sediment interval that corresponds to the opal-A-to-opal-CT transformation at Sites 261, 765, and 766.

Pyrite and Diagenetic Carbonate Formation

Pyrite is a common mineral in most of the Lower Cretaceous sediments from the northwestern Australian margin (Heggie, this volume). Organic matter degradation by sulfate-reducing bacteria produces H_2S, which can react with reduced iron to form pyrite (Berner, 1970, 1984). Organic matter content is highest in rapidly deposited Neocomian sediments. Organic matter is largely of marine origin, but includes varying amounts of terrigenous organic matter (Heggie et al., this volume). Lower to mid-Cretaceous sediment from Site 766 has significantly more organic carbon and pyrite than at Site 765. The modern, partially depleted, pore-water sulfate concentrations and the presence of barite suggest that sulfate reduction was moderate and sulfate concentrations were not reduced to near-zero, as has been commonly observed in more organic-rich marine sediments (Gieskes, 1981, 1983). Minor-to-trace amounts of dolomite, siderite, rhodochrosite, and possibly ankerite were observed in Lower to mid-Cretaceous sediments (e.g., Dumoulin, this volume), but significant amounts of dolomite were found only in the Miocene sediments at Site 765. The abundant Miocene dolomite at Site 765 appears to be authigenic and may have formed by the recrystallization of redeposited aragonite in sulfate-reducing pore waters (Compton, this volume).

CORRELATION AMONG SITES

Correlation of Argo Abyssal Plain Sites 261 and 765

The basal sediments at Sites 261 and 765 are in contact with oceanic basalt. The oldest sediment recovered at these two sites is Late Jurassic in age, based on a detailed comparative study of the sedimentology and nannofossil biostratigraphy of Sites 261 and 765 (Dumoulin and Bown, this volume). Mineral Association V at Site 261 is similar to the lower portion of mineral Association VI and to mineral Association VII at Site 765 (Fig. 5). Mineral Association IV (Barremian) at Site 261 does not appear to correlate with the mineral association of Barremian age at Site 765 (lower half of mineral Association VI) because the I/S from Site 765 contains less than 10% illite layers, compared with the 20% to 30% illite layers in I/S from Site 261. The difference in clay mineralogy between the two sites may reflect different source areas for the sediments, with Site 261 having a greater detrital clay component. Mineral Association III at Site 261 corresponds to the upper half of mineral Association VI at Site 765 and contains abundant opal-CT and highly smectitic I/S. Mineral Association II at Site 261 corresponds to mineral Association V at Site 765 and contains palygorskite and I/S, with variable amounts of illite layers. Mineral Associations IV, III, and part of II at Site 765 are absent or greatly condensed in the interval of no recovery at Site

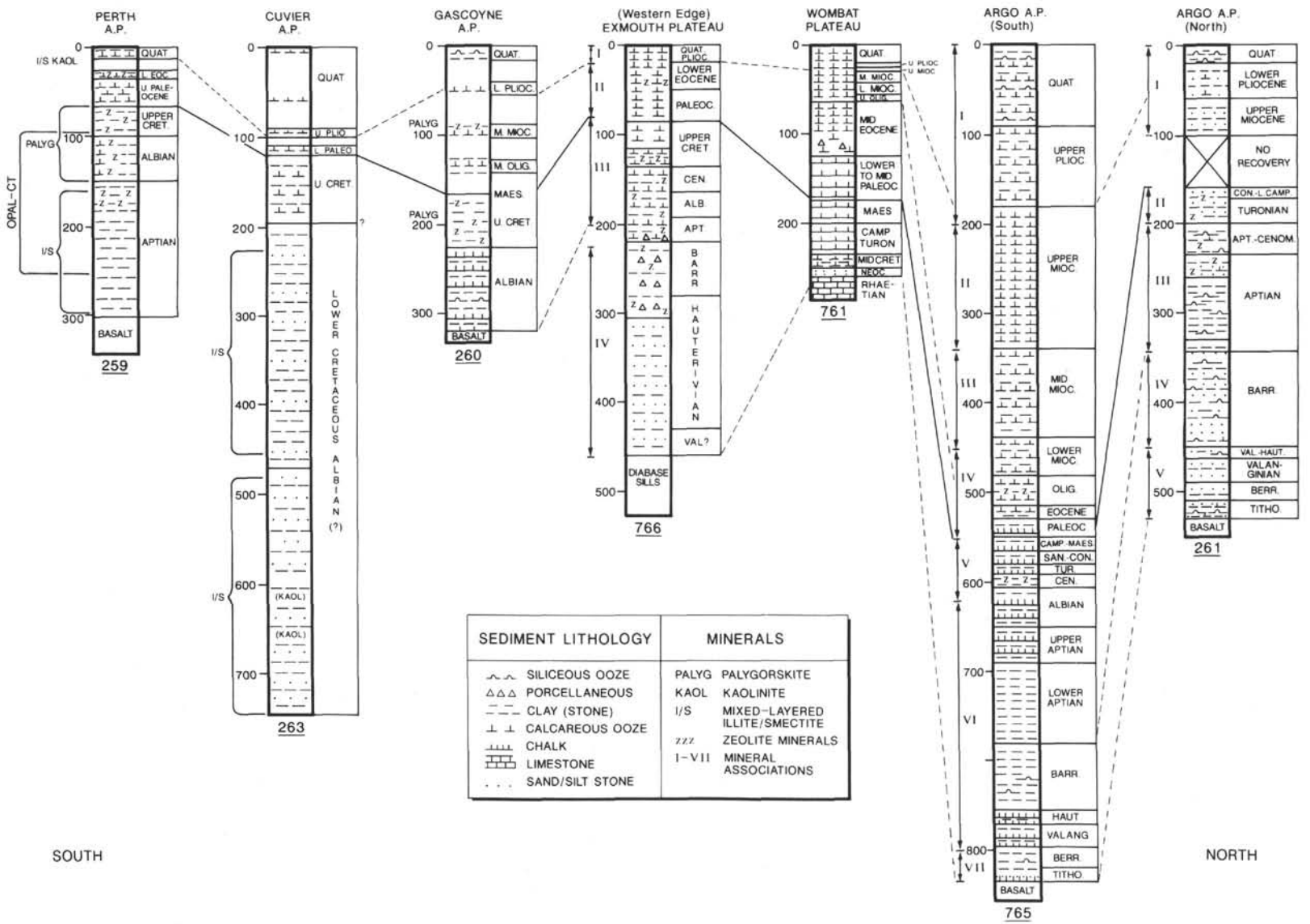

Figure 5. Correlation of depth below seafloor, lithology, age, and mineral associations among sites along the western Australian margin from north (Site 261) to south (Site 259). Roman numerals indicate mineral associations defined in the text.

261. Mineral Association I at Site 261 corresponds to the top of mineral Association II and mineral Association I at Site 765 and consists of detrital I/S and a marked increase in kaolinite. The mineralogy, thickness, and age of sediments at Sites 261 and 765 are fairly similar throughout the Cretaceous (Fig. 5). The major difference in the sedimentation history at Sites 261 and 765 occurs in the Cenozoic, with Site 765 having a much greater thickness of carbonate-rich sediment than Site 261. The thicker Cenozoic sequence at Site 765 is largely the result of the site's closer proximity to a steeper continental rise and slope (Fig. 1). Site 765 is situated at the foot of the continental margin incised by the Swan Canyon that funneled large amounts of reworked calcareous sediment to the Argo Abyssal Plain. Rapid burial of these gravity flows permitted thick sequences of calcareous sediment to accumulate below the CCD. The source area for most of these calcareous turbidites was the adjacent Exmouth Plateau. Although redeposited nannofossils do occur in the lower Pliocene at Site 261, most of the carbonate turbidites at Site 765 did not extend to Site 261. The seismic profile between Sites 261 and 765 indicates that seismic sequences 4, 5, and possibly 6 at Site 765 are absent at Site 261, which agrees with the hiatus indicated in Figure 5 (Buffler, 1990). The cause of this hiatus at Site 261 is unknown, but the hiatus roughly corresponds to the separation of Australia and Antarctica, suggesting that it may have been produced by changes in oceanic circulation, such as intensified bottom-water currents, that resulted from more open-ocean conditions after continental breakup.

Correlation Across the Exmouth Plateau: Sites 765, 761, and 766

The Exmouth Plateau is thought to rest on continental basement; Site 765 rests on oceanic basalt, and Site 766 (on the western edge of the Exmouth Plateau) is thought to have a basement that is intermediate between continental and oceanic (Ludden, Gradstein, et al., 1990). The Exmouth Plateau had a long period of nondeposition from the Rhaetian to the Neocomian that is thought to be a result of subaerial exposure and erosion (von Rad et al., 1989). Neocomian sediment at Site 766 (mineral Association IV) correlates with the lower half of mineral Association VI at Site 765, and with a thin deltaic sandstone unit on the Wombat Plateau. The condensed Tithonian-Berriasian section on the Exmouth Plateau consists of a transgressive belemnite sandstone (von Rad and Thurow, in press). The rapidly deposited Neocomian sediment at Site 766 is thought to be derived from proximal continental source areas that prograded westward into the juvenile Indian Ocean (von Rad et al., 1989). Biomarker and pyrolysis geochemistry at Site 766 indicate that the organic matter is primarily of marine origin, but has a terrigenous component that derived from the nearby continental shelf (Heggie et al., this volume). Basal sandy and silty Hauterivian claystone at Site 766 grades into overlying porcellaneous Barremian claystone. The I/S is highly smectitic and was derived from the alteration of volcanic material. The upper half of mineral Association VI (Aptian) at Site 765 is composed of increasingly calcareous claystone and appears to be absent at Site 766. The Albian to Late Cretaceous mineral Association III at Site 766 correlates with the clayey chalks at Site 761 and with mineral Association V at Site 765. These sediments contain palygorskite and I/S having 20% to 50% illite layers. The Paleocene-to-Eocene mineral Association II at Site 766 correlates to the base of mineral Association IV at Site 765. These sediments are composed of highly smectitic I/S and zeolite minerals. Much of the calcareous sediment at Site 765 was redeposited from the Exmouth Plateau. Northward tilting of the Wombat Plateau during the Jurassic to Early Cretaceous (von Rad et al., 1989) and later formation or enlargement of the Swan Canyon during the Paleogene (Ludden, Gradstein, et al., 1990) reflects increased accelerated gravity flows to the Argo Abyssal Plain during the Cenozoic. The Eocene-to-Pliocene calcareous turbidites of Site 765 are missing from Site 766. These sediments may have bypassed Site 766 in their downslope transport as suggested by the fairly thick Cenozoic carbonate sequence at Site 260 in the adjacent, more distal Gascoyne Abyssal Plain. The Quaternary and Pliocene mineral associations at Site 766 correlate with mineral Association I at Site 765. These predominantly calcareous sediments contain biogenic silica and detrital I/S, mica, and abundant kaolinite derived from the Australian continent.

Correlation of Sites 259, 260, and 263

The sediment sequences recovered at Sites 259 (Perth Abyssal Plain) and 260 (Gascoyne Abyssal Plain) are similar in lithology and mineralogy to sediment recovered at Sites 765 and 766. Both Sites 259 and 260 have a basalt basement overlain by mid-Cretaceous sediment that suggests drifting was younger at these more southern sites (Veevers, Heirtzler, et al., 1974). The sediment sequence at Site 259 is thought to represent deep-water deposits that correlate with shallow-water deposits from the onshore Perth Basin (Veevers and Johnstone, 1974). Carbonate content is high in the Albian, low in the condensed Upper Cretaceous sediment, and high in the Cenozoic. The mid- to Upper Cretaceous sediment at both sites contains palygorskite, zeolite minerals, I/S, and opal-CT. The sediment also contains abundant smectite, but the percent of illite layers in the I/S was not reported (Cooks et al., 1974). Middle Miocene sediment from Site 260 also contains palygorskite and zeolite minerals that correlate with the much thicker Miocene section at Site 765. Radiolarian tests and an increased kaolinite content also have been reported from Quaternary sediments at these sites. Therefore, the mineralogy and diagenetic sequence correlate well along the Australian margin, based on the data available.

Site 263 in the Cuvier Abyssal Plain does not appear to correlate well with the other sites. An unusually thick Lower to mid-Cretaceous sequence was recovered, but basement rock was not reached at Site 263. The Lower to mid-Cretaceous sediment contains abundant coarse-grained continental detritus, including abundant kaolinite and mica. No opal-CT, palygorskite, or zeolite minerals were observed in sediment from Site 263, and radiolarian tests were rare or absent (Cooks et al., 1974). The sequence at Site 263 is proposed as a part of the Winning Group that extends eastward onto the Australian continent. The sediment at Site 263 was probably deposited in a shallow marine environment that later subsided to greater water depths (Veevers and Johnstone, 1974). Therefore, Site 263 appears to have received mostly continental detritus and only minor amounts of pelagic sediment. This may explain why the mineralogy and diagenetic sequence observed at all the other sites were not observed at Site 263.

Regional Correlation

The stratigraphy and mineralogy of sediments recovered from DSDP Leg 27 and ODP Legs 122 and 123 are compared in Figure 5. In general, sediment from the northwestern margin of Australia can be divided into three parts, based on its mineralogy, lithostratigraphy, and biostratigraphy: (1) a Lower Cretaceous (Neocomian) silty and sandy claystone that contains quartz-replaced radiolarian tests and highly smectitic I/S, (2) a mixture of calcareous and clayey siliceous mid- to Upper Cretaceous (Aptian to Maestrichtian) sediment that consists of palygorskite and detrital I/S having a large and variable percentage of illite layers, and (3) Cenozoic sediment that is composed of mostly nannofossil chalk and ooze, except at Site 261, where the Cenozoic section is mostly clay. The three sediment intervals described above can be interpreted to document the juvenile-to-mature evolution of the Indian

Ocean, as discussed by Robinson et al. (1974), Veevers and Johnstone (1974), and von Rad et al. (1989).

The early drifted basin that formed the incipient Indian Ocean was probably a narrow basin having limited circulation and communication with the open ocean. Neocomian sediments are absent from the southern and western sites, suggesting that drifting started in the northwest and migrated to the southwest (Veevers and Heirtzler, 1974). Texturally immature, coarse-grained basal sediments having an abundant volcaniclastic component at Sites 261, 765, and 766 were probably derived locally from the Australian continental margin. The abundance of radiolarian tests suggests high-productivity surface waters. Radiolarian tests are abundant throughout the Cretaceous section but are rare-to-absent in the Cenozoic sequence, except during Quaternary time. The presence of calcareous nannofossils, belemnites, calcispheres, and mollusk shells suggests that these sites were initially above the CCD (Ludden, Gradstein, et al., 1990). The volcanism anticipated during the rift-to-drift transition is supported by the abundance of highly smectitic I/S clay minerals that are interpreted as having derived from the alteration of volcanic material. Bentonite layers were identified in the Lower Cretaceous sediments at Sites 765 and 766 and on the Exmouth Plateau (von Rad and Thurow, in press). It appears that illitization of smectite has occurred in the basal sediments at Site 765 (Compton and Locker, this volume), and illitization may explain the higher percentage of illite layers (20% to 30%) observed in the basal sediments at Sites 261 and 766. Alternatively, the higher percentage of illite layers may reflect a greater detrital I/S component of these sediments.

While the basin continued to widen as the continents drifted apart, cooling of the oceanic lithosphere resulted in thermal subsidence of the passive margin to water depths below the CCD and in increased circulation and communication with the open ocean. The overall mid- to Late Cretaceous sedimentation rates decreased, perhaps because of less continental detritus from lower continental relief and less volcanism, as well as a rise in eustatic sea level, making the sites increasingly distal and starved of terrigenous sediment (Robinson et al., 1974; von Rad et al., 1989). Sedimentation of biogenic silica decreased, and highly smectitic I/S gave way to more detrital I/S during the Late Cretaceous. Pelagic carbonate sedimentation dominated the Cenozoic, except at sites below the CCD that did not receive abundant calcareous turbidites, such as Site 261. Pelagic carbonate productivity may have been enhanced in the Cenozoic because of the more open-ocean conditions produced by the break-up of Australia and Antarctica during the Paleocene and Eocene (Robinson et al., 1974). The abundance of smectite (in places as bentonite layers) and zeolite minerals at most sites in Paleocene and Eocene sediment suggests a renewed source of volcaniclastics.

The thickness of the Cenozoic section is highly variable, and periods of nondeposition occur at many of the sites. For example, the Neogene section at Site 765 is 10 times thicker than that at Site 761, is completely absent at Site 766, and appears to be largely absent at Site 261. However, Cenozoic sediment is poorly represented in Leg 27 sites because of poor recovery and because sites were specifically selected on topographic highs, where the Cenozoic section was thin (Veevers, Heirtzler, et al., 1974). The presence of shallow-water benthic foraminifers, graded bedding, and hiatuses on the continental margin that correspond to rapidly deposited abyssal carbonates indicate that much of the pelagic carbonate originally deposited on the continental margin above the CCD was redeposited by gravity flows to abyssal sites (Ludden, Gradstein, et al., 1990). Therefore, the thickness of the Cenozoic section at abyssal sites depends largely on how near these sites are to steep continental margins. Off-margin transport largely occurred during lowstands of sea level (Dumoulin, this volume).

CONCLUSIONS

1. Sediment from the western Australian continental margin records the progressive juvenile-to-mature evolution of a segment of the Indian Ocean. The mineral associations defined at each site are generally correlative among all of the sites studied over distances of hundreds of kilometers. The mineralogy of basal Neocomian sediment reflects the early stages of formation of the Indian Ocean. Coarse-grained, immature terrigenous sediment, dominated by volcaniclastics, was supplied from the adjacent continental margins. The abundance of highly smectitic mixed-layered illite/smectite was derived from the alteration of terrigenous volcanic material and from ash deposits associated with active spreading. Abundant radiolarian tests that have been altered to quartz and are associated with barite suggest that the narrow incipient basin had highly productive surface waters as a result of upwelling or fluvial nutrient influxes. Degradation of marine and terrigenous organic matter resulted in the formation of pyrite and of trace amounts of diagenetic carbonates (dolomite, rhodochrosite, and siderite).

2. The transition from a juvenile to a mature ocean setting is reflected in an increased abundance of pelagic carbonate sediment during slow sedimentation from the mid- (Aptian/Albian) to Late Cretaceous. Highly smectitic mid-Cretaceous sediment contains abundant opal-CT and zeolite minerals, whereas the overlying Upper Cretaceous sediment contains palygorskite and zeolite minerals that occur only in places. Paleogene sediment is dominated by highly smectitic I/S and contains abundant zeolite.

3. Pelagic carbonate sediment dominates the Neogene and Quaternary, except at abyssal sites that did not receive abundant calcareous turbidites. The noncarbonate fraction contains detrital aluminosilicates (discrete illite, I/S, and kaolinite) that were derived from the Australian continent and biogenic silica (opal-A), but diagenetic sepiolite, palygorskite, and dolomite were only observed in the Miocene sediments at Site 765.

ACKNOWLEDGMENTS

This study was funded by USSAC post-cruise support to J. Compton. We thank Tim Bralower, David Piper, and Ulrich von Rad for their useful comments and suggestions.

REFERENCES

Berger, W. H., and von Rad, U., 1972. Cretaceous and Cenozoic sediments from the Atlantic Ocean. *In* Hayes, D. E., Pimm, A. C., et al., *Init. Repts. DSDP*, 14: Washington (U.S. Govt. Printing Office), 787–954.

Berner, R. A., 1970. Sedimentary pyrite formation. *Am. J. Sci.*, 268:1–23.

_____, 1984. Sedimentary pyrite formation: An update. *Geochim. Cosmochim. Acta*, 48:605–615.

Buffler, R. T., 1990. Underway geophysics. *In* Ludden, J. N., Gradstein, F. M., et al., 1990. *Proc. ODP, Init. Repts.*, 123: College Station, TX (Ocean Drilling Program), 13–25.

Chamley, H., and Millot, G., 1975. Observations sur la répartition et la genèse des attapulgites plio-quaternaires de Mediterranée. *C. R. Hebd. Seances Acad. Sci.*, 281:1215–1218.

Compton, J. S., in press. Clay mineral diagenesis in the Monterey Formation, Santa Maria basin area, California. *Clays Clay Miner.*

Cooks, H. E., Zemmels, I., and Matti, J. C., 1974. X-ray mineralogy data, eastern Indian Ocean—Leg 27, Deep Sea Drilling Project. *In* Veevers, J. J., Heirtzler, J. R., et al., *Init. Repts. DSDP*, 27: Washington (U.S. Govt. Printing Office), 535–548.

Couture, R. A., 1977. Composition and origin of palygorskite-rich and montmorillonite-rich zeolite-containing sediments from the Pacific Ocean. *Chem. Geol.*, 19:113–130.

Eberl, D., and Hower, J., 1976. Kinetics of illite formation. *Geol. Soc. Am. Bull.*, 87:1326–1330.

Gieskes, J. M., 1981. Deep-sea drilling interstitial water studies: implications for chemical alteration of the oceanic crust, layers I and II. *In* Warme, J. E., Douglas, R. G., and Winterer, E. L. (Eds.), *The Deep*

Sea Drilling Project: A Decade of Progress. Spec. Publ.—Soc. Econ. Paleontol. Mineral., 32:149–167.

_____, 1983. The chemistry of interstitial waters of deep-sea sediments: interpretation of Deep-Sea Drilling data. *In* Riley, J. P., and Chester, R. (Eds.), *Chemical Oceanography* (Vol. 8): London (Academic Press), 222–269.

Hay, R. L., 1963. Stratigraphy and zeolitic diagenesis of the John Day Formation of Oregon. *Geol. Sci.*, 42:199–262.

Hower, J., Eslinger, E. V., Hower, M. E., and Perry, E. A., 1976. Mechanism of burial metamorphism of argillaceous sediments: 1. Mineralogical and chemical evidence. *Geol. Soc. Am. Bull.*, 87:725–737.

Iijima, A., 1978. Geological occurrences of zeolite in marine environments. *In* Sand, L. B., and Mumpton, F. A., (Eds.), *Natural Zeolites Occurrence, Properties, Use:* Oxford (Pergamon Press), 175–198.

Jones, J. B., and Segnit, E. R., 1971. The nature of opal. I. Nomenclature and constituent phases. *J. Geol. Soc. Aust.*, 18:56–68.

Kastner, M., 1981. Authigenic silicates in deep-sea sediments: formation and diagenesis. *In* Emiliani, C. (Ed.), *The Sea* (Vol. 7): New York (Wiley), 915–980.

Kastner, M., Keene, J.B., and Gieskes, J.M., 1977. Diagenesis of siliceous oozes. I. Chemical controls on the rate of opal-A to opal-CT transformation—an experimental study. *Geochim. Cosmochim. Acta*, 41: 1041–1059.

Ludden, J. N., Gradstein, F. M., et al., 1990. *Proc. ODP, Init. Repts.*, 123: College Station, TX (Ocean Drilling Program).

Moore, D. M., and Reynolds, R. C., Jr., 1989. *X-Ray Diffraction and the Identification and Analysis of Clay Minerals:* New York (Oxford Univ. Press).

Perry, E. A., Jr., and Hower, J., 1970. Burial diagenesis of the Gulf Coast pelitic sediments. *Clays Clay Miner.*, 18:195–177.

Peterson, M.N.A., Edgar, N. T., von der Borch, C. C., and Rex, R. W., 1970. Cruise leg summary and discussion. *In* Peterson, M.N.A., Edgar, N. T., et al., *Init. Repts. DSDP*, 2: Washington (U.S. Govt. Printing Office), 413–427.

Reynolds, R. C., Jr., 1980. Interstratified clay minerals. *In* Brindley, G. W., and Brown, G. (Eds.), *Crystal Structures of Clay Minerals and their X-Ray Identification.* Mineral. Soc. London Monogr., 5:249–303.

Reynolds, R. C., Jr., and Hower, J., 1970. The nature of interlayering in mixed-layer illite-montmorillonites. *Clays Clay Miner.*, 18:25–36.

Riech, V., and von Rad, U., 1979. Silica diagenesis in the Atlantic Ocean: diagenetic potential and transformations. *In* Talwani, M., Hay, W., and Ryan, W.B.F. (Eds.), *Deep Drilling Results in the Atlantic Ocean: Continental Margins and Paleoenvironment.* Am. Geophys. Union, Maurice Ewing Ser., 3:315–340.

Robinson, P. T., Thayer, P. A., Cook, P. J., and McKnight, B. K., 1974. Lithology of Mesozoic and Cenozoic sediments of the eastern Indian Ocean, Leg 27, Deep Sea Drilling Project. *In* Veevers, J. J., Heirtzler, J. R., et al., *Init. Repts. DSDP*, 27: Washington (U.S. Govt. Printing Office), 1001–1048.

Schmitz, B., 1987. Barium, equatorial high productivity, and the northward wandering of the Indian continent. *Paleoceanography*, 2:63–77.

Stonecipher, S. A., 1976. Origin, distribution, and diagenesis of deep-sea clinoptilolite and phillipsite in deep-sea sediments. *Chem. Geol.*, 17:307–318.

Veevers, J. J., and Heirtzler, J. R., 1974. Tectonic and paleogeographic systhesis of Leg 27. *In* Veevers, J. J., Heirtzler, J. R., et al., *Init. Repts. DSDP*, 27: Washington (U.S. Govt. Printing Office), 1049–1054.

Veevers, J. J., and Johnstone, M. H., 1974. Comparative stratigraphy and structure of the western Australian margin and the adjacent deep ocean floor. *In* Veevers, J. J., Heirtzler, J. R., et al., *Init Repts. DSDP*, 27: Washington (U.S. Govt. Printing Office), 571–585.

von Rad, U., Riech, V., and Rösch, H., 1977. Silica diagenesis in continental margin sediments off northwest Africa. *In* Lancelot, Y., Seibold, E., et al., *Init. Repts. DSDP*, 41: Washington (U.S. Govt. Printing Office), 879–905.

von Rad, U., and Rösch, H., 1972. Mineralogy and origin of clay minerals, silica and authigenic silicates in Leg 14 sediments. *In* Hayes, D. E., Pimm, A. C., et al., *Init. Repts. DSDP*, 14: Washington (U.S. Govt. Printing Office), 727–746.

von Rad, U., and Thurow, J., in press. Bentonitic clays as indicators of early Neocomian post-breakup volcanism off NW Australia (ODP Leg 122). *In* von Rad, U., Haq, B. U., et al., *Proc. ODP, Sci. Results*, 122: College Station, TX (Ocean Drilling Program).

von Rad, U., Thurow, J., Haq, B. U., Gradstein, F., Ludden, J., and ODP Leg 122/123 Shipboard Scientific Parties, 1989. Triassic to Cenozoic evolution of the NW Australian continental margin and the birth of the Indian Ocean (preliminary results of ODP Legs 122 and 123). *Geol. Rundsch.*, 78:1189–1210.

Weaver, C. E., and Beck, K. C., 1977. Miocene of the S.E. United States: a model for chemical sedimentation in a peri-marine environment. *Sediment. Geol.*, 17:1–234.

Date of initial receipt: 12 September 1990
Date of acceptance: 13 June 1991
Ms 123B-113